

Catalytic Mechanism of L,D-Transpeptidase 2 from *Mycobacterium tuberculosis* Described by a Computational Approach: Insights for the Design of New Antibiotics Drugs

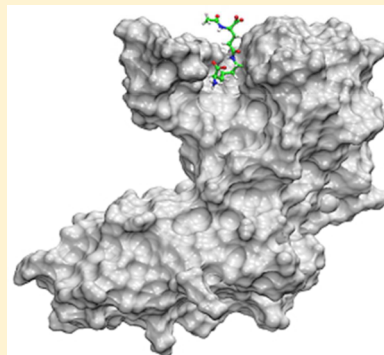
José Rogério A. Silva,^{†,‡,§} Adrian E. Roitberg,^{*,‡,§} and Cláudio Nahum Alves^{*,†,‡,§}

[†]Laboratório de Planejamento e Desenvolvimento de Fármacos, Instituto de Ciências Exatas e Naturais, Universidade Federal do Pará, Belém, PA 66075-110, Brazil

[‡]Department of Chemistry and [§]Quantum Theory Project, University of Florida, Gainesville, Florida 32611, United States

S Supporting Information

ABSTRACT: Tuberculosis is perhaps the most persistent human disease caused by an infections bacterium, *Mycobacterium tuberculosis*. The L,D-transpeptidase enzyme catalyzes the formation of 3 → 3 peptidoglycan cross-links of the *Mtb* cell wall and facilitates resistance against classical β -lactams. Herein, the experimentally proposed mechanism for Ldt_{Mt2} was studied by performing QM/MM MD simulations. The whole mechanistic process includes two stages: acylation and deacylation. During the acylation step, two steps were observed: the first step is a thiolate/imidazole ion-pair in the zwitterionic form, and the second step is the nucleophilic attack on the carboxyl carbon of the natural substrate accompanied by the breaking of the peptide bond on substrate. In the deacylation step the acyl-enzyme suffers a nucleophilic attack on the carboxyl carbon by the amine group of the second substrate. Our free energy results obtained by PMF analysis reveal that the first step (acylation) is the rate-limiting step in the whole catalytic mechanism in accordance with the experimental proposal. Also, the residues responsible for binding of the substrate and transition state stabilization were identified by energy decomposition methods.



INTRODUCTION

Tuberculosis (TB) is an infectious disease caused by an infections bacterium, *Mycobacterium tuberculosis* (*Mtb*). In 2012, an estimated 8.6 million people developed TB and 1.3 million died from the disease.¹ In recent years, multidrug-resistant (MDR) and extensively drug-resistant (XDR) strains of *M. tuberculosis* have appeared as major public health problem that threatens progress made in TB medical care and control worldwide.^{2,3} Drug resistance can arise due to improper use of antibiotics in chemotherapy of drug-susceptible TB patients.^{4,5} The development of new anti-TB drugs is urgently required.⁶

One of the most effective therapeutic classes of antibacterial is β -lactam.⁷ This class of antibacterial compounds inhibits D,D-transpeptidases activity of enzymes commonly referred to as penicillin binding proteins,^{7–9} which are responsible by the most common type of cross-link, the (D,D) 4 → 3 linkage. A second type of cross-link, the (L,D) 3 → 3 linkage, is catalyzed by L,D-transpeptidases (Ldt). The L,D-transpeptidase enzyme catalyzes the formation of 3 → 3 peptidoglycan cross-links of the *M. tuberculosis* cell wall and facilitates resistance against classical β -lactams,¹⁰ such as, penicillins, which inhibit 4,3-transpeptidase activity in *M. tuberculosis*.^{11,12} Carbapenems have been reported to inhibit L,D-transpeptidase activity.^{12–16} Both transpeptidase enzymes need to be inhibited simultaneously to inhibit biosynthesis of the peptidoglycan layer and, consequently, kill the bacteria.

Recently, the X-ray structure of the extra-cellular portion of a *Mtb* L,D-transpeptidase (ex-Ldt_{Mt2}; residues 120–408) was published¹³ and, more recently, a crystal structure of Ldt_{Mt2} in complex with the Meropenem inhibitor was also reported.¹⁷ Ldt_{Mt2} is the enzyme that generates 80% of the transpeptide linkages in *M. tuberculosis* and represent an attractive target for *M. tuberculosis*.^{10,18} For L,D-transpeptidase enzymes two different catalytic mechanism proposals were published so far. The first one was proposed by Biarrote-Sorin and co-workers,¹⁹ the authors proposed that in L,D-transpeptidase, the two paths to the catalytic cysteine (via inner or the outer cavity) are used: one for the acyl donor and the other for the acyl-acceptor substrates. The most recent proposal was suggested by Erdemli and co-workers.¹³ This catalytic mechanism for L,D-transpeptidase is based on cysteine proteases mechanism. Of these, the Erdemli proposal has the much simpler path for the catalytic mechanism, compared to the Biarrote-Sorin proposal, where the enzyme would need to go through several conformational changes of the flap to accommodate entrance of substrates and release of products using the catalytic site channel.¹⁹ In the cysteine protease proposal for Ldt_{Mt2}, the catalytic mechanism occurs in two stages. In the first stage (acylation step), the catalytic Cys352 thiolate formed by proton abstraction attacks the acyl carbon of the substrate and forms a

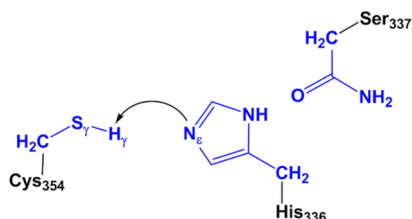
Received: May 21, 2014

Published: August 22, 2014

tetrahedral intermediate. After intermediate thioester formation and protonation by His336 imidazolium group, D-Ala is released. In second stage (deacylation step), another peptide stem enters the catalytic site, also through the external vestibule and binds to catalytic site residues with the side chain amide of the m-A₂pm^{3'} residue (which is isomorphous to D-Ala and also has a D chiral center). In this step His336 acts as a catalytic base by abstracting a proton from the amine group of the m-A₂pm^{3'} residue, while the same amine group performs a nucleophilic attack into carbonyl carbon of acyl-enzyme.¹³

A recent computational study involving the papain enzyme, a member of cysteine protease family, shows that the acylation step is preceded by Cys-thiolate/His-imidazolium formation in its zwitterionic form.²⁰ In this way, in our computational approach, the acylation step proposed by Erdemli¹³ was carried out using cys-thiolate/His-imidazolium formation in its zwitterionic form as starting point for whole catalytic mechanism (see Scheme 1).

Scheme 1. Proposed Mechanism for the Proton Transfer from Neutral Form of Cys354-His336 to Zwitterionic Form^a



^aAtoms in blue are treated by the QM method.

Here, we present a theoretical study aimed to clarify the reaction mechanism of the L,D-transpeptidase of *M. tuberculosis* (Ldt_{Mt2}). We used hybrid quantum mechanic/molecular mechanic (QM/MM) molecular dynamic (MD) simulations to study the details of the catalytic mechanism of Ldt_{Mt2}. Hybrid QM/MM approaches combined with MD simulations have been employed for large-scale studies such as protein-inhibitors interaction and enzymatic catalytic mechanism.^{21–31} In the QM/MM methodology, one part of the system is described by quantum mechanics and the rest by a classical force field.^{21,22} We used the scc-DFTB method³² to describe the QM part of the system. The DFTB method has not only

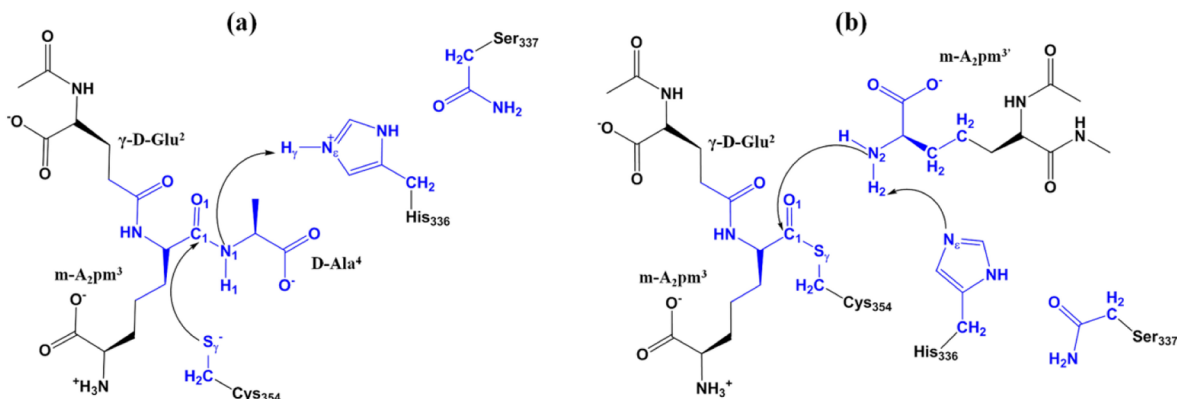
been shown to be an accurate level of theory for describing the energetic of chemical reactions,³³ but it was also demonstrated for biological systems that minimum energy path results are also in good agreement with higher levels of theory like MP2.³⁴ Also, this level of theory produced excellent results for calculations involving pK_a in solution and protein.³⁵ An umbrella sampling technique using an adequate reaction coordinate was employed in order to obtain the free energy profile associated with the catalytic mechanism of Ldt_{Mt2}. In addition, a detailed analysis of the stabilization pattern of the active site residues on the transition states (TSs), in relation to the Michaelis complex (MC) and intermediates (INT1 and INT1') is evaluated by obtaining the energy decomposition.

MATERIALS AND METHODS

Preparation of the Initial Structure. The initial coordinates of ex-Ldt_{Mt2} was obtained from the Protein Data Bank (PDB accession code 3TUR),¹³ which contain a bound peptidoglycan fragment. In our computational analysis, the peptidoglycan fragment was exchanged, in silico, for natural the substrate whose geometry was optimized by performing ab initio quantum mechanical calculations at the HF/6-31G* level of theory using the GAUSSIAN09 package.³⁶ Then, in order to prepare the enzyme-substrate (ES) complex system for MD simulations and free energy calculations, an accurate assignment of the protonation states of all these residues at pH 7 was performed by recalculating the standard pK_a values of the titratable amino acids using the empirical propKa program of Li et al.³⁷ Hydrogen atoms were added to the system using the Leap module as implemented in AMBER12 molecular dynamics package.³⁸ The system was solvated in a truncated octahedral cell of TIP3P³⁹ water molecules, extending 10 Å outside the protein on each side. The AMBER force field 99SB⁴⁰ and the general AMBER force field (GAFF)⁴¹ were employed to describe the protein and natural substrate, respectively. The RESP method was used to calculate the substrate charges applying HF/6-31G* level of theory using GAUSSIAN09 package.³⁶

The enzyme-substrate (ES) complex was initially energy-minimized by carrying out a minimization (5000 steps of each steepest descent and conjugate gradient method) and then gradually heated to 300 K over 2000 ps with a weak constrain of 10 kcal·mol⁻¹·Å⁻² applied to the protein and substrate. The system was relaxed for 100 ps with weak restraints on the solute

Scheme 2. Proposed Mechanism for (a) Acylation Step and (b) Deacylation Step in the Catalytic Site of the Ldt_{Mt2} Enzyme^a



^aAtoms in blue are treated by the QM method.

followed by 200 ps of constant pressure equilibration at 300 K. All minimizations and equilibration steps simulations employed a nonbonded cutoff of 8 Å. The particle mesh Ewald (PME) method was applied to calculate the long-range Coulomb forces. The time step was set to 2 fs, and all bonds involving hydrogen atoms were constrained using the SHAKE algorithm⁴² during the MD simulations.

For hybrid QM/MM MD calculations with ES and INT1' (described later) complex systems, the atoms of the Cys354, His336, Ser337 and natural substrate (in ES complex), and m-A²pm^{3'} substrate (in INT1'), were selected as the QM region, that contains 60 atoms for ES complex and 63 atoms for INT1' complex. The self-consistent charge density functional tight binding (scc-DFTB) Halmiltonian,³² as implemented in AMBER12,⁴³ was employed to describe the QM region, while the rest of the system (protein plus water molecules) was described using the AMBER force field 99SB⁴⁰ and TIP3P³⁹ force fields, respectively, as described early. To satisfy the valence of the QM fragments when the QM-MM boundary divides a covalent bond in all part of QM system, the link atom method was used.⁴⁴

As shown in Scheme 2a and b, the Ldt_{Mt2} catalytic mechanism proposal includes acylation and deacylation stages. The D-Ala leaves the system after the acylation stage. Consequently, we constructed the structure of INT1' by removing the D-Ala out of the QM/MM-equilibrated INT1 structure and adding the second substrate. The constructed and solvated INT1' structure was then relaxed by performing same energy minimization procedure used for ES complex system.

Umbrella Sampling and Free Energy Profile. The free energy profile for the proton transfer in Cys354-thiolate/His336-imidazolium ion pair was evaluated in three different systems. One of them corresponds to a model containing only the catalytic residues Cys354, His336, and Ser337 main chain in a water box. To build this model, we started from the Ldt_{Mt2} crystal structure, cut the bonds linking the Cα atoms to the protein backbone, and then filled the free valence of each Cα with hydrogen atoms. During the MD simulations, a 100 kcal·mol⁻¹·Å⁻² harmonic restraint on the Cα atom for the Cys354/His336 ion pair and Ser337 main chain was applied to their starting positions so as to maintain the same distances as in the enzyme environment. The water molecules were modeled by MM while Cys354-His336-Ser337 residues were part of the QM system (see Scheme 1). The other two systems were the apo and holo form of Ldt_{Mt2} enzyme. For the holo form case, the natural substrate was also considered part of QM system, as described previously.

The proton transfer reaction coordinate was defined as the distance between the proton that is transferred and the acceptor nitrogen, RC = $d(S_{\gamma}-H_{\gamma}) - d(H_{\gamma}-N_{\epsilon})$. This RC was sampled from -1.50 to 1.50 Å, the scans were done in steps of 0.20 Å. The reaction coordinate for acylation step was chosen as proposed by Wei and co-workers in a previous free energy study for papain cysteine protease,²⁰ the acylation step is represented by a nucleophilic attack on the carbonyl group of the substrate by the S_γ of Cys354 side chain, accompanied by the proton (H_γ) transfer for N_ε atom of His336 to the N₁ atom of the substrate and the breaking of C₁-N₁ bond of the substrate. The structural change from intermediate INT1 to intermediate INT2 (acylation step) involves the breaking of the C₁-N₁ and H_γ-N_ε bonds, and the formation of S_γ-C₁ and N₂-H_γ bonds. Then, the acylation reaction coordinate step was described as RC = $d(C_1-N_1) + d(H_{\gamma}-N_{\epsilon}) - d(S_{\gamma}-C_1) -$

$d(N_2-H_{\gamma})$ (see Scheme 2a). This RC was sampled from -7.00 to 4.00 Å in steps of 0.20 Å.

For the deacylation step, starting from the equilibrate INT2' structure (see Scheme 2b), the nucleophilic attack on the carbonyl group of the covalent intermediate by the N₂ of m-A²pm^{3'} substrate, accompanied by the proton (H₂) transfer for N₂ atom of m-A²pm^{3'} substrate to N_ε atom of His336 and the breaking of S_γ-C₁ bond of the covalent intermediate. Then, the deacylation reaction coordinate step was described as RC = $-d(C_1-N_2) + d(N_2-H_2) - d(N_{\epsilon}-H_2)$ (see Scheme 2b). This RC was sampled from -6.40 to 2.50 Å, the scans were done in steps of 0.20 Å.

In each window, 10 ps of equilibration were followed by 20 ps of production with a time step of 1.0 fs. The last structure of each MD in a given umbrella window was used as the initial one to perform the next one for which the value of the reaction coordinate is restrained to the next position. All QM/MM MD simulations were performed constraining the value of the RC with harmonic potential using a force constant of 100.0 kcal·mol⁻¹·Å⁻². The probability density and the free energy profile for the unbiased system along the reaction coordinates were obtained applying the variational free energy profile (VFEP)⁴⁵ implemented in the VFEP program developed by Lee and co-workers.^{45,46}

Interaction Energy Decomposition. In order to analyze how the active site residues stabilize/destabilize the acylation and deacylation stages in the reaction catalyzed by Ldt_{Mt2}, we used the energy decomposition method. This method has been extensively applied to enzymatic systems.⁴⁷⁻⁵¹ The influence of an individual residue side-chain on the energy of a determined structure or state is measured taking into account the difference of energies when a particular residue is present (named by *i* in eq 1) or when it is mutated to Gly (*i* - 1 in eq 1).^{52,53}

$$\Delta E_i = [E_i^{\text{QM}} + E_i^{\text{QMMM}}] - [E_{i-1}^{\text{QM}} + E_{i-1}^{\text{QMMM}}] \quad (1)$$

where each term in brackets means the energy of the QM part influenced by the classical environment. Then, the differences between the stabilization effects in going from reactant to TS, for each residue, was estimated by

$$\Delta \Delta E_i = \Delta E_i^{\text{TS}} - \Delta E_i^{\text{reactant}} \quad (2)$$

In our analysis, the QM subsystem was composed of the substrates, Cys354, His336, and Ser337, as indicated in Schemes 2a and b, for acylation and deacylation stages, respectively. To obtain the average values for the interaction energy and stabilization effects of each residue in a particular state, 50 snapshots from QM/MM MD simulations were considered. They were taken from umbrella sampling calculation with reaction coordinates corresponding to the reactant and its respective transition state.

RESULTS AND DISCUSSION

Proton Transfer Analysis. The standard pK_a values of cysteine and histidine residues are about 9.1 and 6.4 in solution, respectively.⁵⁴ However, kinetic studies on different thiol proteases showed that there are two ionizable groups forming part in the catalysis, one with pK_a around 4 and another with a pK_a around 8.5.^{55,56} The former is usually attributed to the deprotonation of the thiol group of cysteine, whereas the latter is believed to reflect the ionization of the imidazolium group of histidine. The large observed pK_a shifts prove the strong influence of the enzymatic environment. Moreover, the

cysteine/histidine pair has been shown to exist in this zwitterionic form already in the ground state of cysteine proteases.^{55,56} A simple transformation for the shifted ΔpK_a into ΔG_r° provides an estimate of about $-6.20 \text{ kcal}\cdot\text{mol}^{-1}$, showing that the proton transfer from Cys354-thiolate group to His336-imidazolium group is likely to happen in protein environment. The ΔG_r° obtained in our study for the Cys354-thiolate/His336-imidazolium ion pair model in apo form (without substrate) was $-10.00 \text{ kcal}\cdot\text{mol}^{-1}$, confirming the fact mentioned above and in somewhat good agreement with the simple estimate from the individual pK_a s. Similar results were found in previous computational studies.⁵⁷ Considering the water system, the ΔG_r° is $-32 \text{ kcal}\cdot\text{mol}^{-1}$ smaller than apo form, indicating that that proton transfer is more likely to happen in water solution at pH 7 when the same protein distance is maintained in water solution. For the holo form (with substrate), results show that reactants (Cys354SH/His336) and products (Cys354S⁻/His336H⁺) are still way, where the ΔG_r° found was $-29.00 \text{ kcal}\cdot\text{mol}^{-1}$, indicating that in holo form the Cys354-thiolate/His336-imidazolium formation is more likely to happen than in apo form.

The free energy profiles for these three systems discussed above are shown in Figure 1. Several studies show the

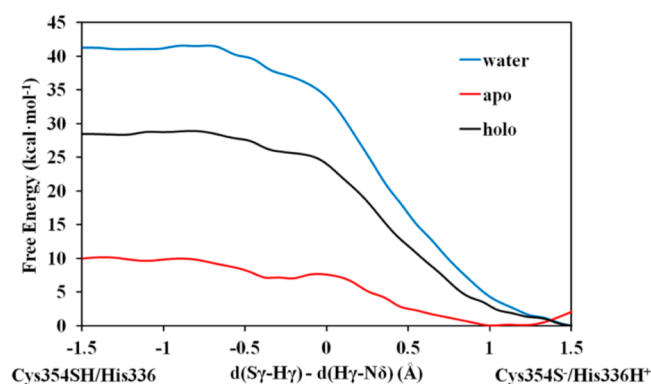


Figure 1. Free energy profile for the proton transfer from Cys354 to His336 in the model system (blue) and in the apo (red) and holo (black) form of the Ldt_{Mt2} enzyme. The reactant state corresponds to the left side of the graphic.

importance of pK_a values of specific residues for catalytic enzymatic mechanism.^{35,51,54,58–62} In most cases, these changes are motivated by enzymatic environment. Here, in all discussed systems Cys354S⁻/His336H⁺ is shown to be more stable than its neutral form (Cys354SH/His336).

Free Energy Profile for Acylation and Deacylation Steps. The QM/MM umbrella sampling calculations have revealed that the fundamental Ldt_{Mt2} catalytic mechanism consists of two reaction steps after Cys354-thiolate/His336-imidazolium ion pair formation: acylation and deacylation steps, respectively. Michaelis complex (MC), the product of the proton transfer from Cys354 to His336, is considered as the starting point for the acylation step. Here, we have three major types of structural changes. One is the formation of S_γ–C₁ bond, the $d(S_\gamma-C_1)$ decreases from 4.10 Å in MC to 2.46 Å in transition state (TS1) and then to 1.90 Å in intermediate (INT1), indicating the nucleophilic attack of thiolate group of Cys354 to carbonyl carbon of substrate (C₁). The second significant structural change is the breaking of C₁–N₁ bond, the $d(C_1-N_1)$ increases from 1.37 Å in MC to 1.53 Å in TS1 and then to 2.80 Å in INT1, indicating the peptide bond break of

substrate. The other is the proton (H_γ) transfer from N_ε atom of His336 side chain to the N₁ atom of the substrate, the $d(N_1-H_\gamma)$ and $d(N_\epsilon-H_\gamma)$ respectively change from 3.74 and 1.08 Å in MC complex to 1.19 and 1.50 Å in TS1, and then to 1.02 and 3.32 Å in INT1. All these distance and their standard deviations are summarized in Table 1. Interestingly, the H_δ atom of

Table 1. Averaged of Key Distances for MC, TS1, and INT1 Structures for Acylation Step (Å) Obtained by DFTB/MM 1D-PMF^a

DFTB/MM	MC	TS1	INT1
$d(S_\gamma-C_1)$	4.10 (0.18)	2.46 (0.12)	1.90 (0.05)
$d(C_1-N_1)$	1.37 (0.02)	1.53 (0.06)	2.80 (0.10)
$d(N_1-H_\gamma)$	3.74 (0.20)	1.19 (0.06)	1.02 (0.02)
$d(N_\epsilon-H_\gamma)$	1.08 (0.04)	1.50 (0.13)	3.32 (0.13)

^aAll standard deviation values in parentheses.

His336 maintains a strong hydrogen-bonding interaction with the carbonyl oxygen of residue Ser337 in the whole acylation stage. This interaction stabilizes the protonated tautomer of His336, in accordance with experimental observations.¹³

As can be seen from Scheme 2b, D-Ala was removed from the above-discussed QM/MM obtained geometry of the intermediate INT1 to construct the structure of the intermediate INT1', which was the relaxed by performing MD simulation as explained in the Materials and Methods section. The D-Ala was, in silico, changed to the m-A²pm^{3'} substrate. Starting from the equilibrated INT1' structure, our QM/MM reaction-coordinate calculations revealed that the deacylation stage consists of a concerted mechanism, which is in accordance with previous theoretical studies for cysteine proteases.^{20,30,57,63} For this stage, accompanied by the nucleophilic attack on the carbonyl carbon C₁ in the covalent intermediate by the N₂ atom of A²pm^{3'} substrate, the proton (H₂) transfers from the N₂ atom of m-A²pm^{3'} to the N_ε atom of residue His336 to form the product (PROD) state via transition state TS2. Hence, the deacylation step involves breaking of N₂–H₂ bond and the formation of C₁–N₂ and N_ε–H₂ bonds, beyond of resulting break of S_γ–C₁ bond. Here, the $d(S_\gamma-C_1)$, $d(N_2-C_1)$, $d(N_2-H_2)$, and $d(N_\epsilon-H_2)$ distances change respectively from 1.90, 2.78, 1.02, and 3.24 Å in intermediate INT1' to 2.13, 1.85, 1.30, and 1.30 Å in transition state TS2, and then to 3.80, 1.36, 3.58, and 1.02 Å in PROD state. All of these distances and their standard deviations are summarized in Table 2.

The activation free energy obtained by DFTB/MM simulations observed between MC and TS1 is $32.00 \text{ kcal}\cdot\text{mol}^{-1}$ for the acylation step (Figure 2a and b). In addition, the energy barrier between INT1' and TS2, which corresponds to the deacylation step is $28.25 \text{ kcal}\cdot\text{mol}^{-1}$ (Figure 3a and b).

Table 2. Averaged of Key Distances for INT1', TS2, and PROD Structures for Deacylation Step (Å) Obtained by DFTB/MM 1D-PMF^a

DFTB/MM	INT1'	TS2	PROD
$d(S_\gamma-C_1)$	1.90 (0.05)	2.13 (0.15)	3.80 (0.20)
$d(N_2-C_1)$	2.78 (0.13)	1.85 (0.14)	1.36 (0.02)
$d(N_2-H_2)$	1.02 (0.02)	1.30 (0.06)	3.58 (0.06)
$d(N_\epsilon-H_2)$	3.24 (0.15)	1.30 (0.07)	1.02 (0.02)

^aAll standard deviation values in parentheses.

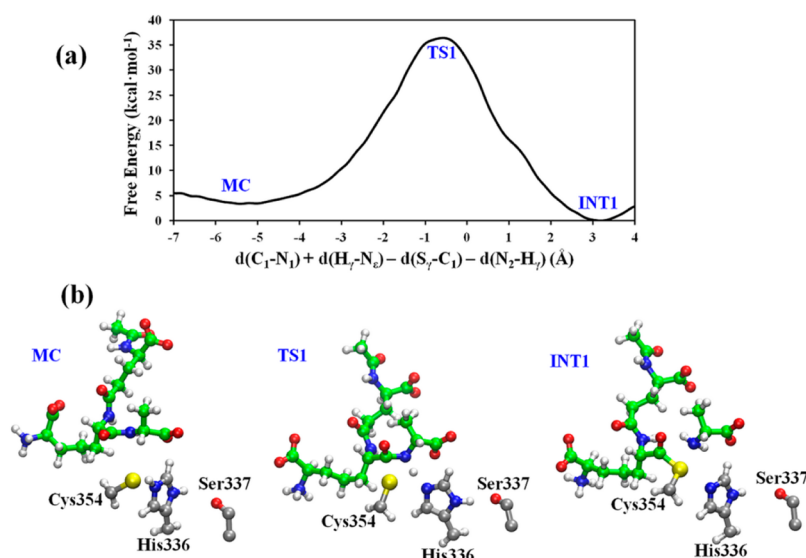


Figure 2. (a) Free energy profile for the acylation step of Ldt_{Mt2} enzyme. The reactant state corresponds to the left side of the graphics. (b) 3D structures of reactant (MC), transition state (TS1), and product (INT1) for acylation step of the Ldt_{Mt2} enzyme.

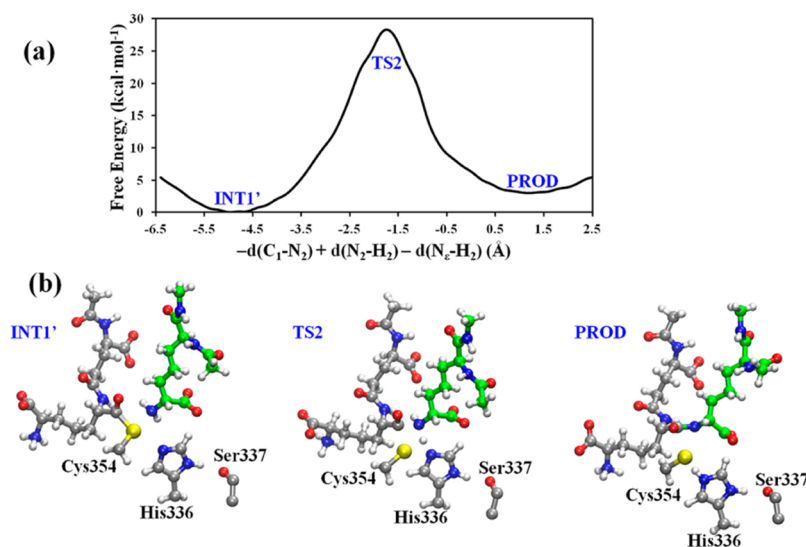


Figure 3. (a) Free energy profile for the deacylation step of Ldt_{Mt2} enzyme. The reactant state corresponds to the left side of the graphics. (b) 3D structures of reactant (INT1'), transition state (TS2), and product (PROD) for deacylation step of the Ldt_{Mt2} enzyme.

Although DFTB shows high energy values for free energy barriers,^{33,64–66} our results are consistent with the experimental observation that the acylation stage is rate-limiting for cysteine protease enzymes.^{20,30,63}

Besides, an interesting structural change found in the system for both acylation and deacylation stages reflects the importance of the β -hairpin flap that covers the catalytic site in Ldt_{Mt2} ¹³ and Ldt_{fm} ⁶⁷ enzymes. Our MD simulation results suggest that this β -hairpin flap is responsible for accommodating and covering the substrate during the acylation step (see Figure S1). This structural behavior was not identified in the deacylation step, since the covalent intermediate is already accommodating the enzyme catalytic site (see Figure S2). Also, it can explain the reason that the acylation step is considered rate-limiting for whole catalytic mechanism.

Interaction Energy Decomposition. The origin of the substrate-enzyme interaction can be analyzed by decomposing the total interaction energy and taking into account the

difference in energies when a particular residue is mutated, as described in the Materials and Methods section. In order to get a deeper insight into protein–substrate interactions, we used 50 snapshots from the QM/MM MD simulations taken from umbrella sampling calculation, for all substrate–protein complexes appearing along each free energy profile: MC and TS1 for acylation step; INT1' and TS2 for deacylation step. Figure 4a and b shows how the main amino acid residues interact in the active site. Averaged protein–substrate interaction energies by residue in this acylation/deacylation complex and relative stabilization pattern on transition state with respect to the respective reactant are displayed in Figure 5a and b. The addition over all the $\Delta\Delta E$ values for each residue represents an indication of the degree of the stabilization for each TS from the enzyme environment in the QM subsystem (Figure 5a). In Figure 5a, a negative value means a stabilizing effect on the TS and positive value means as destabilizing effect of a give residue on the TS.

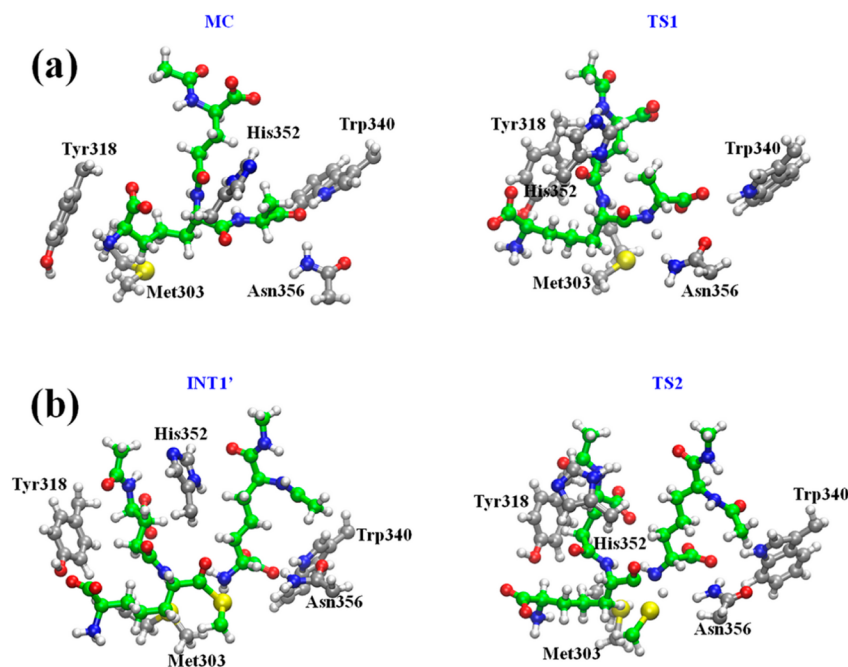


Figure 4. 3D structures and amino acid residues considered on residual decomposition analysis for (a) acylation step and (b) deacylation step of the Ldt_{Mt2} enzyme.

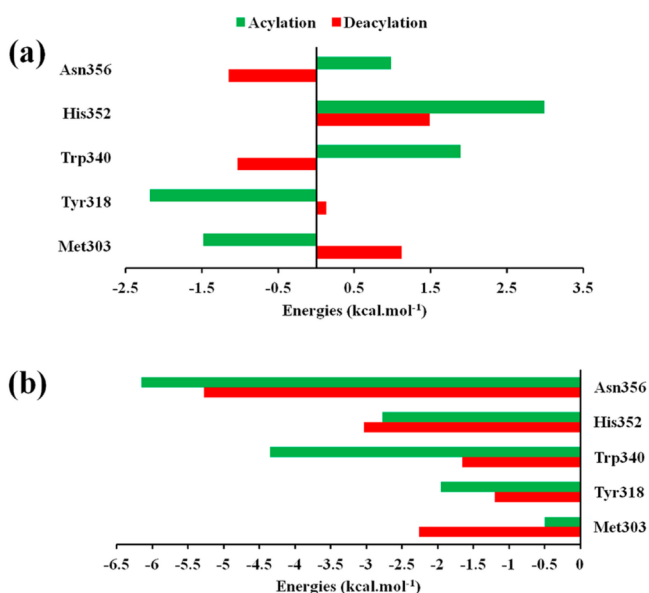


Figure 5. (a) Relative stabilization (eq 2) of the active site residues for the acylation (green) and deacylation (red) steps on the catalytic mechanism of the Ldt_{Mt2} enzyme. (b) Binding residual energy of the active site residues for the acylation (green) and deacylation (red) steps on the catalytic mechanism of the Ldt_{Mt2} enzyme.

The residues Met303, Tyr318, Trp340, His352, and Asn356 are experimentally identified as important residues for natural substrate binding.¹³ Using computational tools we can identify their contributions along the reaction mechanism. In order to quantify the interactions performed by these residues, the energy decomposition method was carried out. As we can see in Figure 5a, the residual contribution for above residues shows opposite character, which it is expected once that acylation and deacylation steps are opposite reactions. For the acylation step the Tyr318 and Met303 residues show stabilizing effects for the

transition state (TS1), which is in agreement with the experimental proposal where, mainly the Tyr318 residue is responsible for recognizing the D chiral center of the diamino acid side chain of the substrate. Meanwhile, the residues Trp340, His352 and Asn356 show stabilizing effects for the reactant state (Michaelis complex), namely, they are more important for the binding substrate (Figure 5b). Particularly, the His352 and Asn356 residues are responsible for stabilizing the departing of the D-Ala amide on the acylation step and proving further recognition of the donor stem L chiral center. Only, the His353 residue shows a similar character for both acylation and deacylation stages, it has the similar energy value in substrate binding energy (Figure 5b), since the L chiral center for in the leaving group of the acylation step and nucleophilic group of the deacylation step are similar. These factors contribute to understanding the importance of each residue selected experimentally, which can be used to propose new Ldt_{Mt2} inhibitors.

Insights for Design of New Antibiotics Drugs. Some experimental studies have proposed β -lactam as a class of antibiotics that inhibit the polymerization of cell wall peptidoglycan.^{6,7,11,15,16,18,67,68} Carbapenems compounds belong to subfamily of β -lactam inhibitors that irreversibly inhibit classical D,D-transpeptidase enzymes.^{7,16} Erdemli and co-workers¹³ used calorimetric studies to determine the inhibition values for two potent Ldt_{Mt2} inhibitors: imipenem and Meropenem. In other recent experimental study, the crystal structure of Ldt_{Mt2} in complex with Meropenem was elucidated.¹⁷ Some residues are listed as key for Meropenem inhibitory activity, besides the catalytic triad (Cys354-His336-Ser337) responsible by bond cleaves on the inhibitor; Tyr308 and Tyr318 are pointed to as essential residues for flipping the inhibition mechanism. In our study, the Tyr318 residue shows important influence in stabilization of the acylation transition state and experimentally it is responsible for recognizing the D chiral center of the diamino acid side chain of the substrate.¹³

Some inhibitors are generally built to resemble the structure of a molecular species occurring during the chemical reaction and, in particular, transition states or intermediates structures, if we accept the seminal hypothesis of Pauling that enzymes catalyze reactions by preferentially binding (and stabilizing) the transition state.⁶⁹ In our case, the β -lactam compounds can be compared to TS1 of Ldt_{Mt2} catalytic mechanism. In this way, new and more potent inhibitors can be proposed using the similar factors occurring in β -lactam compounds and TS1 or other molecular species found during the chemical reaction. Then, we proposed a procedure where the structural and energetic values are taking into account to design new Ldt_{Mt2} inhibitors: (a) performing molecular docking calculations to predict the initial conformation of the new compound using as reference the transition state structure obtained by QM/MM umbrella sampling calculations; (b) a molecular dynamics simulations should be performed in order to equilibrate and provide an ensemble of structures of the complex; (c) to calculate binding free energy for each complex ensemble and to correlate this value with energy obtained for catalytic mechanism. If the new compound has lower value than found on residual analysis in the catalytic mechanism for transition state, this new compound should be a more potent inhibitor for Ldt_{Mt2} enzyme. Finally, with that said energy values determinate by our theoretical approach can be considered to propose new carbapenem compounds with higher Ldt_{Mt2} activity.

CONCLUSIONS

In this paper, the enzymatic catalytic mechanism of L,D-transpeptidase of *M. tuberculosis* has been described by means of umbrella sampling calculations using an hybrid DFTB/MM potential. The results have allowed us to obtain a complete profile of the possible reaction path corresponding to the acylation and deacylation steps involved in the whole mechanism. According to our results, the Cys354-thiolate/His336-imidazolium pair formation is the starting point to drive the acylation step. Then, the attack of Cys354 on the carbonyl carbon of the substrate would take place in a single step corresponding to the formation of the covalent intermediate. This is step rate-limiting, in agreement with experimental data for cysteine proteases. In the second step of the whole mechanism (deacylation step), the amine group of the second substrate attacks the acyl-enzyme complex and then the 3 \rightarrow 3 peptide bond is formed. A thorough analysis of the substrate–protein interactions reveals the importance of some of the residues, such as Met303, Tyr318, Trp340, His352, and Asn356, in anchoring the substrate in a proper orientation for the reaction to take place. Finally, it is important to stress that our simulations have allowed detection of two different dynamical behavior of a β -hairpin flap that cover the catalytic site in Ldt_{Mt2} which can explain the barrier energy difference found in acylation and deacylation step. Thus, these results may be useful for the rational design of new compounds with higher inhibitory activity against *M. tuberculosis* bacillus.

ASSOCIATED CONTENT

Supporting Information

Figures S1 and S2 as well as videos S1 and S2. This material is available free of charge via the Internet at <http://pubs.acs.org>.

AUTHOR INFORMATION

Corresponding Authors

*Phone: (352) 392-6972. Fax: (352) 392-8722. E-mail: roitberg@ufl.edu.

*Phone: (+55) 91-3201-8235. Fax: (+55) 91-3201-7633. E-mail: nahum@ufpa.br.

Notes

The authors declare no competing financial interest.

ACKNOWLEDGMENTS

We gratefully acknowledge financial support from *Conselho Nacional de Desenvolvimento Científico e Tecnológico (CNPq)*. J.R.A.S. and C.N.A. thank *Coordenação de Aperfeiçoamento de Pessoal de Nível Superior (CAPES)* for financial support. The authors acknowledge the University of Florida Research Computing for providing computational resources and support that have contributed to the research results reported in this publication. We also thank Justin Smith for the corrections and suggestions in English that helped to improve this study.

REFERENCES

- (1) WHO. *Global Tuberculosis Report*; Geneva, 2013.
- (2) Fauci, A. S.; Grp, N. T. W. Multidrug-resistant and extensively drug-resistant tuberculosis: The National Institute of Allergy and Infectious Diseases research agenda and recommendations for priority research. *J. Infect. Dis.* **2008**, *197*, 1493–1498.
- (3) Gandhi, N. R.; Nunn, P.; Dheda, K.; Schaaf, H. S.; Zignol, M.; van Soolingen, D.; Jensen, P.; Bayona, J. Multidrug-resistant and extensively drug-resistant tuberculosis: a threat to global control of tuberculosis. *Lancet* **2010**, *375*, 1830–1843.
- (4) Jindani, A.; Dore, C. J.; Mitchison, D. A. Bactericidal and sterilizing activities of antituberculosis drugs during the first 14 days. *Am. J. Respir. Crit. Care Med.* **2003**, *167*, 1348–1354.
- (5) Lewis, K. Persister cells, dormancy and infectious disease. *Nat. Rev. Microbiol.* **2007**, *5*, 48–56.
- (6) Koul, A.; Arnoult, E.; Lounis, N.; Guillemont, J.; Andries, K. The challenge of new drug discovery for tuberculosis. *Nature* **2011**, *469*, 483–490.
- (7) Fisher, J. F.; Meroueh, S. O.; Mobashery, S. Bacterial resistance to beta-lactam antibiotics: Compelling opportunism, compelling opportunity. *Chem. Rev.* **2005**, *105*, 395–424.
- (8) Tipper, D. J. Stroming, J. L. Mechanism of action of penicillins - a proposal based on their structural similarity to acyl-d-alanyl-d-alanine. *Proc. Natl. Acad. Sci. U.S.A.* **1965**, *54*, 1133–1141.
- (9) Tipper, D. J. Mode of action of beta-lactam antibiotics. *Pharmacol. Ther.* **1985**, *27*, 1–35.
- (10) Lavollay, M.; Arthur, M.; Fourgeaud, M.; Dubost, L.; Marie, A.; Veziris, N.; Blanot, D.; Gutmann, L.; Mainardi, J.-L. The peptidoglycan of stationary-phase *Mycobacterium tuberculosis* predominantly contains cross-links generated by L,D-transpeptidation. *J. Bacteriol.* **2008**, *190*, 4360–4366.
- (11) Gupta, R.; Lavollay, M.; Mainardi, J.-L.; Arthur, M.; Bishai, W. R.; Lamichhane, G. The *Mycobacterium tuberculosis* protein Ldt-(Mt2) is a nonclassical transpeptidase required for virulence and resistance to amoxicillin. *Nat. Med.* **2010**, *16*, 466–U22.
- (12) Nolan, S. T.; Lamichhane, G. Protective Efficacy of BCG Overexpressing an L, D-Transpeptidase against *M. tuberculosis* Infection. *PLoS One* **2010**, *5*, e13773–e13780.
- (13) Erdemli, S. B.; Gupta, R.; Bishai, W. R.; Lamichhane, G.; Amzel, L. M.; Bianchet, M. A. Targeting the Cell Wall of *Mycobacterium tuberculosis*: Structure and Mechanism of L,D-Transpeptidase 2. *Structure* **2012**, *20*, 2103–2115.
- (14) Triboulet, S.; Arthur, M.; Mainardi, J.-L.; Veckerle, C.; Dubee, V.; Nguekam-Moumi, A.; Gutmann, L.; Rice, L. B.; Hugonnet, J.-E. Inactivation Kinetics of a New Target of beta-Lactam Antibiotics. *J. Biol. Chem.* **2011**, *286*, 22777–22784.

- (15) Haenni, M.; Moreillon, P.; Lazarevic, V. Promoter and transcription analysis of penicillin-binding protein genes in *Streptococcus gordonii*. *Antimicrob. Agents Chemother.* **2007**, *51*, 2774–2783.
- (16) Veziris, N.; Truffot, C.; Mainardi, J.-L.; Jarlier, V. Activity of Carbapenems Combined with Clavulanate against Murine Tuberculosis. *Antimicrob. Agents Chemother.* **2011**, *55*, 2597–2600.
- (17) Li, W.-J.; Li, D.-F.; Hu, Y.-L.; Zhang, X.-E.; Bi, L.-J.; Wang, D.-C. Crystal structure of L,D-transpeptidase Ldt(Mt2) in complex with Meropenem reveals the mechanism of carbapenem against *Mycobacterium tuberculosis*. *Cell Res.* **2013**, *23*, 728–731.
- (18) Lamichhane, G. Novel targets in *M. tuberculosis*: search for new drugs. *Trends Mol. Med.* **2011**, *17*, 25–33.
- (19) Biarrotte-Sorin, S.; Hugonnet, J. E.; Delfosse, V.; Mainardi, J. L.; Gutmann, L.; Arthur, M.; Mayer, C. Crystal structure of a novel beta-lactam-insensitive peptidoglycan transpeptidase. *J. Mol. Biol.* **2006**, *359*, 533–538.
- (20) Wei, D.; Huang, X.; Liu, J.; Tang, M.; Zhan, C.-G. Reaction Pathway and Free Energy Profile for Papain-Catalyzed Hydrolysis of N-Acetyl-Phe-Gly 4-Nitroanilide. *Biochemistry* **2013**, *52*, 5145–5154.
- (21) Rosta, E.; Klahn, M.; Warshel, A. Towards accurate ab initio QM/MM calculations of free-energy profiles of enzymatic reactions. *J. Phys. Chem. B* **2006**, *110*, 2934–2941.
- (22) Warshel, A.; Levitt, M. Theoretical studies of enzymic reactions - dielectric, electrostatic and steric stabilization of carbonium-ion in reaction of lysozyme. *J. Mol. Biol.* **1976**, *103*, 227–249.
- (23) Senn, H. M.; Thiel, W. QM/MM Methods for Biomolecular Systems. *Angew. Chem., Int. Ed.* **2009**, *48*, 1198–1229.
- (24) Marti, S.; Andres, J.; Moliner, V.; Silla, E.; Tunon, I.; Bertran, J. Computational design of biological catalysts. *Chem. Soc. Rev.* **2008**, *37*, 2634–2643.
- (25) van der Kamp, M. W.; Mulholland, A. J. Combined Quantum Mechanics/Molecular Mechanics (QM/MM) Methods in Computational Enzymology. *Biochemistry* **2013**, *52*, 2708–2728.
- (26) Ruiz-Pernia, J. J.; Silla, E.; Tunon, I.; Marti, S. Hybrid quantum mechanics/molecular mechanics simulations with two-dimensional interpolated corrections: Application to enzymatic processes. *J. Phys. Chem. B* **2006**, *110*, 17663–17670.
- (27) Pierdominici-Sottile, G.; Horenstein, N. A.; Roitberg, A. E. Free Energy Study of the Catalytic Mechanism of Trypanosoma cruzi trans-Sialidase. From the Michaelis Complex to the Covalent Intermediate. *Biochemistry* **2011**, *50*, 10150–10158.
- (28) Reis, M.; Alves, C. N.; Lameira, J.; Tunon, I.; Marti, S.; Moliner, V. The catalytic mechanism of glyceraldehyde 3-phosphate dehydrogenase from Trypanosoma cruzi elucidated via the QM/MM approach. *Phys. Chem. Chem. Phys.* **2013**, *15*, 3772–3785.
- (29) Araujo Silva, J. R.; Lameira, J.; Alves, C. N. Insights for design of Trypanosoma cruzi GAPDH inhibitors: A QM/MM MD study of 1,3-bisphospho-D-glyceric acid analogs. *Int. J. Quantum Chem.* **2012**, *112*, 3398–3402.
- (30) Harrison, M. J.; Burton, N. A.; Hillier, I. H. Catalytic mechanism of the enzyme papain: Predictions with a hybrid quantum mechanical molecular mechanical potential. *J. Am. Chem. Soc.* **1997**, *119*, 12285–12291.
- (31) Mladenovic, M.; Fink, R. F.; Thiel, W.; Schirmeister, T.; Engels, B. On the origin of the stabilization of the zwitterionic resting state of cysteine proteases: A theoretical study. *J. Am. Chem. Soc.* **2008**, *130*, 8696–8705.
- (32) Elstner, M.; Porezag, D.; Jungnickel, G.; Elsner, J.; Haugk, M.; Frauenheim, T.; Suhai, S.; Seifert, G. Self-consistent-charge density-functional tight-binding method for simulations of complex materials properties. *Phys. Rev. B: Condens. Matter Mater. Phys.* **1998**, *58*, 7260–7268.
- (33) Woodcock, H. L.; Hodoscek, M.; Brooks, B. R. Exploring SCC-DFTB paths for mapping QM/MM reaction mechanisms. *J. Phys. Chem. A* **2007**, *111*, 5720–5728.
- (34) Barnett, C. B.; Naidoo, K. J. Ring Puckering: A Metric for Evaluating the Accuracy of AM1, PM3, PM3CARB-1, and SCC-DFTB Carbohydrate QM/MM Simulations. *J. Phys. Chem. B* **2010**, *114*, 17142–17154.
- (35) Riccardi, D.; Schaefer, P.; Cui, Q. pK(a) calculations in solution and proteins with QM/MM free energy perturbation simulations: A quantitative test of QM/MM protocols. *J. Phys. Chem. B* **2005**, *109*, 17715–17733.
- (36) Frisch, M. J.; Trucks, G. W.; Schlegel, H. B.; Scuseria, G. E.; Robb, M. A.; Cheeseman, J. R.; Scalmani, G.; Barone, V.; Mennucci, B.; Petersson, G. A.; Nakatsuji, H.; Caricato, M.; Li, X.; Hratchian, H. P.; Izmaylov, A. F.; Bloino, J.; Zheng, G.; Sonnenberg, J. L.; Hada, M.; Ehara, M.; Toyota, K.; Fukuda, R.; Hasegawa, J.; Ishida, M.; Nakajima, T.; Honda, Y.; Kitao, O.; Nakai, H.; Vreven, T.; Montgomery, J. A.; Peralta, J. E.; Ogliaro, F.; Bearpark, M.; Heyd, J. J.; Brothers, E.; Kudin, K. N.; Staroverov, V. N.; Kobayashi, R.; Normand, J.; Raghavachari, K.; Rendell, A.; Burant, J. C.; Iyengar, S. S.; Tomasi, J.; Cossi, M.; Rega, N.; Millam, J. M.; Klene, M.; Knox, J. E.; Cross, J. B.; Bakken, V.; Adamo, C.; Jaramillo, J.; Gomperts, R.; Stratmann, R. E.; Yazyev, O.; Austin, A. J.; Cammi, R.; Pomelli, C.; Ochterski, J. W.; Martin, R. L.; Morokuma, K.; Zakrzewski, V. G.; Voth, G. A.; Salvador, P.; Dannenberg, J. J.; Dapprich, S.; Daniels, A. D.; Farkas, Foresman, J. B.; Ortiz, J. V.; Cioslowski, J.; Fox, D. J. *Gaussian 09*; Wallingford, CT, 2009.
- (37) Li, H.; Robertson, A. D.; Jensen, J. H. Very fast empirical prediction and rationalization of protein pK(a) values. *Proteins* **2005**, *61*, 704–721.
- (38) Case, D.; Darden, T. A.; Cheatham, T. E.; Simmerling, C.; Wang, J.; Duke, R.; Luo, R.; Crowley, M.; Walker, R.; Zhang, W.; Merz, K. M.; Wang, B.; Hayik, S.; Roitberg, A.; Seabra, G.; Kolossvary, I.; Wong, K. F.; Paesani, F.; Vanicek, J.; Wu, X.; Brozell, S.; Steinbrecher, T.; Gohlke, H.; Yang, L.; Tan, C.; Mongan, J.; Hornak, V.; Cui, G.; Mathews, D. H.; Seetin, M. G.; Sagui, C.; Babin, V.; Kollman, P., *Amber 12*; University of California: San Francisco, 2012.
- (39) Jorgensen, W. L.; Chandrasekhar, J.; Madura, J. D.; Impey, R. W.; Klein, M. L. Comparison of simple potential functions for simulating liquid water. *J. Chem. Phys.* **1983**, *79*, 926–935.
- (40) Hornak, V.; Abel, R.; Okur, A.; Strockbine, B.; Roitberg, A.; Simmerling, C. Comparison of multiple amber force fields and development of improved protein backbone parameters. *Proteins* **2006**, *65*, 712–725.
- (41) Wang, J. M.; Wolf, R. M.; Caldwell, J. W.; Kollman, P. A.; Case, D. A. Development and testing of a general amber force field. *J. Comput. Chem.* **2004**, *25*, 1157–1174.
- (42) Ryckaert, J. P.; Ciccotti, G.; Berendsen, H. J. C. Numerical-integration of cartesian equations of motion of a system with constraints - molecular-dynamics of n-alkanes. *J. Comput. Phys.* **1977**, *23*, 327–341.
- (43) Seabra, G. d. M.; Walker, R. C.; Elstner, M.; Case, D. A.; Roitberg, A. E. Implementation of the SCC-DFTB method for hybrid QM/MM simulations within the amber molecular dynamics package. *J. Phys. Chem. A* **2007**, *111*, 5655–5664.
- (44) Field, M. J.; Bash, P. A.; Karplus, M. A Combined quantum-mechanical and molecular mechanical potential for molecular-dynamics simulations. *J. Comput. Chem.* **1990**, *11*, 700–733.
- (45) Lee, T.-S.; Radak, B. K.; Pabis, A.; York, D. M. A New Maximum Likelihood Approach for Free Energy Profile Construction from Molecular Simulations. *J. Chem. Theory Comput.* **2013**, *9*, 153–164.
- (46) Lee, T.-S.; Radak, B. K.; Huang, M.; Wong, K.-Y.; York, D. M. Roadmaps through Free Energy Landscapes Calculated Using the Multidimensional vFEP Approach. *J. Chem. Theory Comput.* **2014**, *10*, 24–34.
- (47) Chatfield, D. C.; Eurenus, K. P.; Brooks, B. R. HIV-1 protease cleavage mechanism: A theoretical investigation based on classical MD simulation and reaction path calculations using a hybrid QM/MM potential. *J. Mol. Struct.: THEOCHEM* **1998**, *423*, 79–92.
- (48) Dinner, A. R.; Blackburn, G. M.; Karplus, M. Uracil-DNA glycosylase acts by substrate autocatalysis. *Nature* **2001**, *413*, 752–755.
- (49) Garcia-Viloca, M.; Truhlar, D. G.; Gao, J. L. Reaction-path energetics and kinetics of the hydride transfer reaction catalyzed by dihydrofolate reductase. *Biochemistry* **2003**, *42*, 13558–13575.

- (50) Hensen, C.; Hermann, J. C.; Nam, K. H.; Ma, S. H.; Gao, J. L.; Holtje, H. D. A combined QM/MM approach to protein-ligand interactions: Polarization effects of the HIV-1 protease on selected high affinity inhibitors. *J. Med. Chem.* **2004**, *47*, 6673–6680.
- (51) Pierdominici-Sottile, G.; Roitberg, A. E. Proton Transfer Facilitated by Ligand Binding. An Energetic Analysis of the Catalytic Mechanism of Trypanosoma cruzi Trans-Sialidase. *Biochemistry* **2011**, *50*, 836–842.
- (52) Major, D. T.; Gao, J. A combined quantum mechanical and molecular mechanical study of the reaction mechanism and alpha-amino acidity in alanine racemase. *J. Am. Chem. Soc.* **2006**, *128*, 16345–16357.
- (53) Wong, K.-Y.; Gao, J. The reaction mechanism of paraoxon hydrolysis by phosphotriesterase from combined QM/MM Simulations. *Biochemistry* **2007**, *46*, 13352–13369.
- (54) Harris, T. K.; Turner, G. J. Structural basis of perturbed pK(a) values of catalytic groups in enzyme active sites. *IUBMB Life* **2002**, *53*, 85–98.
- (55) Polgar, L. Spectrophotometric determination of mercaptide ion, an activated form of sh-group in thiol enzymes. *FEBS Lett.* **1974**, *38*, 187–190.
- (56) Polgar, L. Mercaptide - imidazolium ion-pair - reactive nucleophile in papain catalysis. *FEBS Lett.* **1974**, *47*, 15–18.
- (57) Strajbl, M.; Florian, J.; Warshel, A. Ab initio evaluation of the free energy surfaces for the general base/acid catalyzed thiolysis of formamide and the hydrolysis of methyl thioformate: A reference solution reaction for studies of cysteine proteases. *J. Phys. Chem. B* **2001**, *105*, 4471–4484.
- (58) McIntosh, L. P.; Hand, G.; Johnson, P. E.; Joshi, M. D.; Korner, M.; Plesniak, L. A.; Ziser, L.; Wakarchuk, W. W.; Withers, S. G. The pK(a) of the general acid/base carboxyl group of a glycosidase cycles during catalysis: A C-13-NMR study of Bacillus circulans xylanase. *Biochemistry* **1996**, *35*, 9958–9966.
- (59) Vocadlo, D. J.; Davies, G. J.; Laine, R.; Withers, S. G. Catalysis by hen egg-white lysozyme proceeds via a covalent intermediate. *Nature* **2001**, *412*, 835–838.
- (60) Phillips, D. C. Hen egg-white lysozyme molecule. *Proc. Natl. Acad. Sci. U.S.A.* **1967**, *57*, 484–&.
- (61) Zhou, M. M.; Davis, J. P.; Vanetten, R. L. Identification and pK(a) determination of the histidine-residues of human low-molecular-weight phosphotyrosyl protein phosphatases - a convenient approach using an mlev-17 spectral editing scheme. *Biochemistry* **1993**, *32*, 8479–8486.
- (62) Chivers, P. T.; Prehoda, K. E.; Volkman, B. F.; Kim, B. M.; Markley, J. L.; Raines, R. T. Microscopic pK(a) values of Escherichia coli thioredoxin. *Biochemistry* **1997**, *36*, 14985–14991.
- (63) Ma, S.; Devi-Kesavan, L. S.; Gao, J. Molecular dynamics Simulations of the catalytic pathway of a cysteine protease: A combined QM/MM study of human cathepsin K. *J. Am. Chem. Soc.* **2007**, *129*, 13633–13645.
- (64) Kruger, T.; Elstner, M.; Schiffels, P.; Frauenheim, T. Validation of the density-functional based tight-binding approximation method for the calculation of reaction energies and other data. *J. Chem. Phys.* **2005**, *122*, 114110–114114.
- (65) Lundberg, M.; Sasakura, Y.; Zheng, G.; Morokuma, K. Case Studies of ONIOM(DFT:DFTB) and ONIOM(DFT:DFTB:MM) for Enzymes and Enzyme Mimics. *J. Chem. Theory Comput.* **2010**, *6*, 1413–1427.
- (66) Gaus, M.; Cui, Q.; Elstner, M. Density functional tight binding: application to organic and biological molecules. *Wiley Interdiscip. Rev.: Comput. Mol. Sci.* **2014**, *4*, 49–61.
- (67) Lecoq, L.; Dubee, V.; Triboulet, S.; Bougault, C.; Hugonnet, J.-E.; Arthur, M.; Simorre, J.-P. Structure of Enterococcus faecium L,D-Transpeptidase Acylated by Ertapenem Provides Insight into the Inactivation Mechanism. *ACS Chem. Biol.* **2013**, *8*, 1140–1146.
- (68) Dubee, V.; Triboulet, S.; Mainardi, J.-L.; Etheve-Quequejau, M.; Gutmann, L.; Marie, A.; Dubost, L.; Hugonnet, J.-E.; Arthur, M. Inactivation of Mycobacterium tuberculosis L,D-Transpeptidase Ldt-(Mt1) by Carbapenems and Cephalosporins. *Antimicrob. Agents Chemother.* **2012**, *56*, 4189–4195.
- (69) Pauling, L. Nature of forces between large molecules of biological interest. *Nature* **1948**, *161*, 707–709.